Analysis of Hyperspectral Data for Estimation of Temperate Forest Canopy Nitrogen Concentration: Comparison Between an Airborne (AVIRIS) and a Spaceborne (Hyperion) Sensor

Marie-Louise Smith, Mary E. Martin, Lucie Plourde, and Scott V. Ollinger

***Abstract*—Field studies among diverse biomes demonstrate that mass-based nitrogen concentration at leaf and canopy scales is strongly related to carbon uptake and cycling. Combined field and airborne imaging spectrometry studies demonstrate the capacity for accurate empirical estimation of forest canopy N concentration and other biochemical constituents at scales from forest stands to small landscapes. In this paper, we report on the utility of the first space-based imaging spectrometer, Hyperion, for estimation of temperate forest canopy N concentration as compared to that achieved with the airborne high-altitude imaging spectrometer, the Airborne Visible/Infrared Imaging Spectrometer (AVIRIS). Overall accuracy of Hyperion estimates of forest canopy N concentration, as compared with field measurements, were within 0.25% dry mass, and AVIRIS-based estimates were within 0.19% dry mass, each well within the accuracy required to distinguish among forested ecosystems in nitrogen status.**

***Index Terms*—Airborne Visible/Infrared Imaging Spectrometer (AVIRIS), Hyperion, nitrogen, temperate forest.**

I. Introduction

THE CONCENTRATION of nitrogen in foliage is strongly related to rates of net photosynthesis, and hence carbon uptake, across a wide range of plant species and functional groups [1], [2] and thus represents a simple and biologically meaningful link between terrestrial cycles of carbon and nitrogen (N). Field and remote sensing studies in temperate forest ecosystems, employing both laboratory spectroscopy and airborne imaging spectrometry, have demonstrated the capacity for empirical estimation of canopy N and other biochemical constituents (e.g., lignin, cellulose, etc.) at scales from individual leaves to whole forest canopies [3], [4]. In the case of nitrogen, empirical relationships are based on both direct and indirect correlations with absorption features associated with N-bearing compounds in leaves, e.g., proteins and chlorophyll [5], [6]. More recently, this approach has been extended to ecosystem properties that are functionally linked to canopy chemistry including growth and N cycling [7], [8]. In this paper, we compare the capacity of the first spaceborne hyperspectral imaging spectrometer, Hyperion (one instrument on the National Aeronautics and Space Administration (NASA) New Millennium Program Earth Observing-1 platform), for remote empirical estimation of temperate forest canopy N with that achieved using a high-altitude airborne hyperspectral sensor, NASA's Airborne Visible/Infrared Imaging Spectrometer (AVIRIS).

Manuscript received July 2, 2002; revised January 29, 2003. This work was supported in part by the National Aeronautics and Space Administration and via a fellowship to M. L. Smith by the Organization for Economic Cooperation and Development Co-operative Research Programme: Biological Resource Management for Sustainable Agricultural Systems.

M.-L. Smith is with the U.S. Department of Agriculture Forest Service, Northeastern Research Station, Durham, NH 03824 USA (e-mail: marielouisesmith@fs.fed.us).

M. E. Martin, L. Plourde, and S. V. Ollinger are with the Complex Systems Research Center, University of New Hampshire, Durham, NH 03824 USA (e-mail: mary.martin@unh.edu; lucie.plourde@unh.edu; scott.ollinger@unh.edu).

Digital Object Identifier 10.1109/TGRS.2003.813128

II. Methods

A. Study Area

The study was conducted at the Bartlett Experimental Forest [(BEF) W 71.30°, N 44.05°] located in central New Hampshire and within the White Mountain National Forest. Established in 1932 by the U.S. Department of Agriculture's Forest Service, the BEF is a 1052-ha tract of secondary successional needle-leaved evergreen and broad-leaved deciduous forest types including such northern temperate conifer species as red spruce (Picea rubens Sarg.), balsam fir (*Abies balsamea* (L.) Miller), eastern hemlock (*Tsuga candensis* (L.) Carr.), and white pine (*Pinus strobus* L.), as well as such temperate northern hardwood species as sugar maple (*Acer saccharum* Marsh), American beech (*Fagus grandifolia* Ehrh.), yellow birch (*Betula alleghaniensis* (L.) Britt.), red maple (*Acer rubrum* L.), white ash (*Fraxinus americana* L.), and paper birch (*Betula papyrifera* Marsh.). The study area is mountainous with elevations ranging from 200–850 m. Soils are derived from granitic drift and tend to be coarse textured. The climate is characterized by a relatively short growing season (frost-free period of about 120 days) and long cold winters. Air temperatures at the BEF average -12° and 19 °C in January and July, respectively [36]. Precipitation is evenly distributed throughout the year and averages 120–140 cm, with about one-third in the form of snow.

B. Field Data Collection and Chemical Analysis

In 1931, 500 0.1-ha permanent growth measurement plots, spaced 200 m $\times$ 100 m apart, were established across the BEF. Forty-four of these established permanent plots were chosen for canopy composition and foliar chemistry sampling for remote sensing image calibration. Plots were chosen to represent

a broad range in species composition and stand age, and are part of a larger study directed at the application of hyperspectral remote sensing to analysis of canopy chemistry and ecosystem function at stand to landscape scales [7], [8].

In order to determine growing season foliar chemistry, and in conjunction with image acquisition by NASA's AVIRIS and Hyperion instruments, midsummer green leaf samples were collected on each selected study plot in August 1997 and again on 19 of these plots in August 2000. On each plot, all dominant and codominant species were identified, and between two and seven trees per species were selected for green leaf collection. Leaves were collected by shooting small branches from the canopy with a shotgun. Each sample consisted of a composite of leaves collected from several heights in the canopy. For needle-leaved species, no separation was made among needles of different ages. All samples were oven-dried at 70 °C for 48 h and then ground with a Wiley mill to pass through a 1-mm mesh screen.

A visible-near infrared spectrophotometer (NIRSystems 6500 monochromator) was used to determine foliar N concentration of oven-dried, ground green leaf foliage samples according to established methods [9]. As N concentration on a mass basis has been shown not to vary significantly in relation to vertical canopy gradients [10], [11], plot-level whole-canopy N concentration (grams Nitrogen per 100 g) was calculated as the mean of foliar N concentration for individual species in each forest stand, weighted by fraction of canopy foliar mass per species. Each species contribution to the total mass of the canopy was determined by combining its proportional leaf area, determined using a camera-based point quadrat sampling technique, with leaf mass per area measurements. Complete details of the field and lab methodologies are described elsewhere [8], [12].

C. Remote Sensing Data and Image Processing

Cloud-free imaging spectrometer data were acquired for the BEF on August 12, 1997 by the AVIRIS instrument and on August 29, 2001 by the Hyperion instrument.

AVIRIS flies onboard an ER-2 aircraft at an altitude of 20 000 m and measures upwelling radiance from the solar reflected spectrum in 224 contiguous channels from 0.4–2.4 μm with a spectral resolution of 0.01 μm. Spatial images of radiance spectra are collected by a cross-track scanning mechanism and the forward motion of the aircraft. Images are 11 km in width and up to 800 km in length with a nominal spatial resolution of 17 m [13]. AVIRIS data were received as at-sensor scaled radiance (μW cm^{-2} sr^{-1} nm^{-1}) and transformed to apparent surface reflectance using the Atmosphere Removal (ATREM) atmospheric correction program [14], [15]. ATREM was designed specifically for retrieving scaled surface reflectance from spectral image data collected by the AVIRIS sensor. ATREM uses a radiative transfer model based on the MODTRAN and 5S codes to calculate atmospheric transmittance of seven gases, particularly water. Atmospheric attenuation and scattering effects of these gases are then removed from the image on a pixel-by-pixel basis. After atmospheric correction, the BEF AVIRIS image was geometrically registered to within 0.5-pixel accuracy using a geocoded SPOT panchromatic coverage of the study area. AVIRIS reflectance spectra for pixel areas encompassing each sample plot, typically a 2 × 2 pixel area, were extracted for analysis.

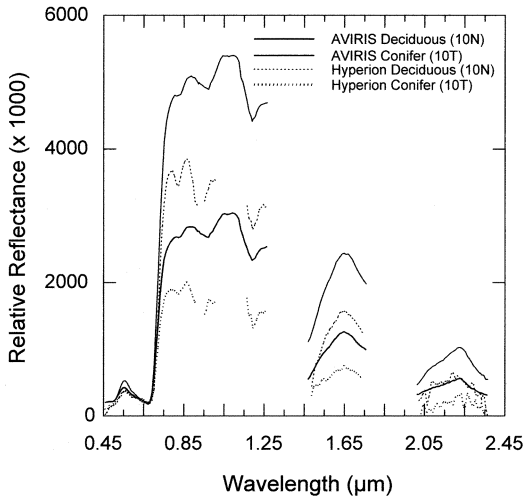

Fig. 1. AVIRIS and Hyperion reflectance spectra for a broad-leaved deciduous (10N) and a needle-leaved evergreen (10T) forest stand, Bartlett Experimental Forest, NH. Solid lines represent AVIRIS spectra, broken lines represent Hyperion spectra.

Hyperion Level 1B data, described in detail elsewhere in this issue [16], were provided as calibrated radiance (W m^{-2} sr^{-1} μm^{-1}). Level 1B Hyperion radiance data were first corrected for "streaking" or variation in balance among vertical columns in the along-track direction of the image data, a product of the sensor's "pushbroom" design, that is most evident in shortwave infrared (SWIR) channels (1.0–2.4 μm). This artifact was treated as scene dependent and corrected using a simple statistical balancing approach using the mean and variance of each column and each channel of image data [17]. Radiance data were then transformed to apparent surface reflectance using the ACORN atmospheric correction program [18]. Similar to ATREM, ACORN is based on the MODTRAN 4 radiative transfer model and calculates the effect of atmospheric gases as well as molecular and aerosol scattering and removes these effects on a pixel-by-pixel basis from the image. After atmospheric correction, the BEF Hyperion image was geometrically registered using the georegistered AVIRIS image of the study site. Hyperion reflectance spectra encompassing both the ground plot area and the ground extent included in AVIRIS analysis were extracted for spectral analysis.

A comparison among AVIRIS and Hyperion reflectance spectra for a broad-leaved deciduous and a needle-leaved evergreen stand is presented in Fig. 1. Although ATREM and ACORN do not produce identical surface reflectance transformations, differences among platforms, instrument SNR, and the temporal offset between AVIRIS and Hyperion data collection are likely larger more significant sources of variation in this analysis.

D. Statistical Analysis

Prior to examination of correlations among spectral data and whole-canopy N concentration, plot-level reflectance spectra (R) were transformed to absorbance (A) where

$$A = \log_{10}(1/R) \tag{1}$$

and a derivative transformation (approximated by finite difference) applied. According to Beer–Lambert, the concentration of an absorber is directly proportional to A where A is the product of molecular absorption, the concentration of absorbers, and the path length of irradiating energy [19]. The derivative spectrum is a measure of the slope of the spectral curve at every point and results in a spectrum in which peaks and valleys correspond with inflection points in the absorbance spectra (thus aiding in resolving overlapping spectral peaks) and from which baseline offsets and low-frequency variation have been removed or minimized [20]. In the case of optically dense vegetation, such as found in closed-canopy forests, the spectral derivative with respect to wavelength can be shown to be directly indicative of the abundance and activity of absorbers in leaves [21].

Wavelength regions associated with overtones of strong water absorption centered near 1.45 and 1.90 μm were excluded from analysis of both AVIRIS and Hyperion data. AVIRIS wavelengths below 0.45 μm and Hyperion wavelengths below 0.45 μm and above 2.0 μm were also excluded from analysis due to low SNR.

Partial least squares (PLS) regression, a type of eigenvector analysis, was used to relate AVIRIS and Hyperion spectral response to whole-canopy N concentration data for each sample stand and was carried out using the Unscrambler 7.6 software system [22]. PLS regression methods reduce full-spectrum data to a smaller set of independent latent variables, or factors, with constituent concentration data used directly during the spectral decomposition process. As a result, full-spectrum wavelength loadings for significant PLS factors $(p < 0.05)$, from which regression coefficients for each wavelength are derived, are directly related to constituent concentration and thus describe the spectral variation most relevant to the modeling of variation in the chemical data [23]. To avoid overfitting, the prediction residual error sum of squares (PRESS) statistic was calculated for each factor based on an iterative cross-validation prediction of each sample. The number of factors at which additive prediction errors are minimized indicates the appropriate number of factors to include in each PLS model.

Derivative transformations were performed iteratively during PLS regression analysis over variable wavelength widths with the aim of maximizing the squared multiple correlation coefficient between spectral data and whole-canopy nitrogen concentration while minimizing the standard error. A number of math treatments were evaluated and are expressed as the order of the derivative, the gap between data points used to calculate the derivative and the number of data points used to smooth the data.

Accuracy of developed equations was evaluated using the residual mean square error of prediction (RMSEP) statistic, based on an iterative calibration–validation algorithm. Each canopy N concentration sample and its associated spectra are iteratively excluded, and a prediction of the sample value is made based on an equation developed using the remaining samples. The process is repeated until every sample has been left out once, and then all prediction residuals are combined to compute the validation equation statistics and RMSEP. The RMSEP is the average prediction error expressed in units of N concentration and is effectively equivalent to the standard error of prediction (SEP) for an independent dataset [23].

TABLE I
RESULTS OF FIELD DATA COLLECTION FROM SAMPLE PLOTS IN 44 FOREST STANDS, BEF

Plot	Predominant Species Composition	Canopy N (g N /100 g)		LAI (m^2 m^{-2})
		1997	*2000*	
36Z	Beech	1.85	1.82	3.49
38Q	Beech	1.87	1.70	3.04
42J	Beech	2.08	1.76	
9J	Beech	2.15		
16L	Beech	2.21		
18T	Beech	2.21		
14J	Beech	2.48		
38U	Beech-Hemlock	1.61		
24T	Beech-Red Maple	2.12		
12J	Beech-Red Oak	2.05		
13J	Beech-Red Oak	2.19		3.33
30G	Paper Birch-Beech	2.26	2.05	
30T	Paper Birch-Beech	2.30	1.85	3.39
28AF	Red Maple	1.99		
23X	Red Maple	2.07		
30Y	Red Maple-Beech	1.76	1.55	3.35
30V	Red Maple-Beech	1.91		
28AB	Red Maple-Paper Birch	1.67		
26V	Red Maple-Paper Birch	1.70		
28AE	Red Maple-White Pine	1.96		
9D	Sugar Maple-Beech	1.88	2.02	3.52
14Z	Sugar Maple-Beech	1.98	2.01	
43J	Sugar Maple-Beech	1.98		
10N	Sugar Maple-Beech	2.03	2.07	
12H	Sugar Maple-Beech	2.15		3.34
6D	Sugar Maple-Beech	2.18		
5D	Sugar Maple-Beech	2.21		
24P	Sugar Maple-White Ash	2.02		3.47
9L	Yellow Birch-Beech	1.98		
9V	Yellow Birch-Beech	2.28		
36G	Yellow Birch-Beech	2.39	2.38	
24I	Hemlock	1.20	1.26	
32V	Hemlock	1.28		
32P	Hemlock	1.30	1.49	3.09
40G	Hemlock	1.35	1.14	
14L	Hemlock-Beech	1.69		
34K	Hemlock-Red Spruce	1.22	1.27	2.78
7V	Red Spruce	1.00		1.73
10T	Red Spruce	1.05	1.16	1.80
7N	Red Spruce	1.11	1.10	1.90
6N	Red Spruce	1.17	1.26	1.82
30AE	Red Spruce-Paper Birch	1.26	1.06	2.58
32AF	White Pine-Mixed Deciduous	1.35	1.35	3.46
32AH	White Pine-Mixed Deciduous	1.64		3.62

III. RESULTS

Table I summarizes plot-level field measurements. Canopy N concentration varied more than twofold across all sites differing in both mean and range among deciduous broad-leaved and needle-leaved evergreen forest types. Among deciduous stands, canopy N concentration ranged from 1.61% to 2.48% in 1997 ($n = 31$ stands, mean $= 2.05\%$) and from 1.55% to 2.38% in 2000 ($n = 10$, mean $= 1.92\%$). Among evergreen-dominated stands canopy N ranged from 1.00% to 1.69% in 1997 ($n = 13$, mean $= 1.28\%$) and from 1.06% to 1.49% in 2000 ($n = 9$, mean $= 1.26\%$). Leaf area index (LAI), a scalar of canopy mass and density, showed greater variation among needle-leaved evergreen-dominated stands (LAI: 1.73 to 3.62, mean 2.53) than among broad-leaved deciduous-dominated stands, largely a function of variation in leaf retention time among diverse conifer species. Within deciduous-dominated stands, canopy N concentration showed greater relative variation than did LAI which varied little (LAI: 3.04 to 3.52, mean 3.37), most stands being at or near maximum LAI values for forests of this region. Fuller discussion may be found in [8].

Although foliar N concentration can vary as much as 20% across several years in temperate forests of this region [24], be-

TABLE II
SUMMARY STATISTICS FOR PLS REGRESSION OF FOREST CANOPY NITROGEN CONCENTRATION WITH AVIRIS AND HYPERION SPECTRAL RESPONSE, BEF

	Math Treatment	Factors	Calibration			
			R^2	*SEC*	*CV*	*Bias*
AVIRIS	1, 4, 3	3	0.83	0.17	0.09	0.00
Hyperion	1, 4, 3	3	0.82	0.17	0.10	0.00
			Validation			
			R^2	*RMSEP*	*CV*	*Bias*
AVIRIS	1, 4, 3	3	0.79	0.19	0.10	0.00
Hyperion	1, 4, 3	3	0.60	0.25	0.15	0.00

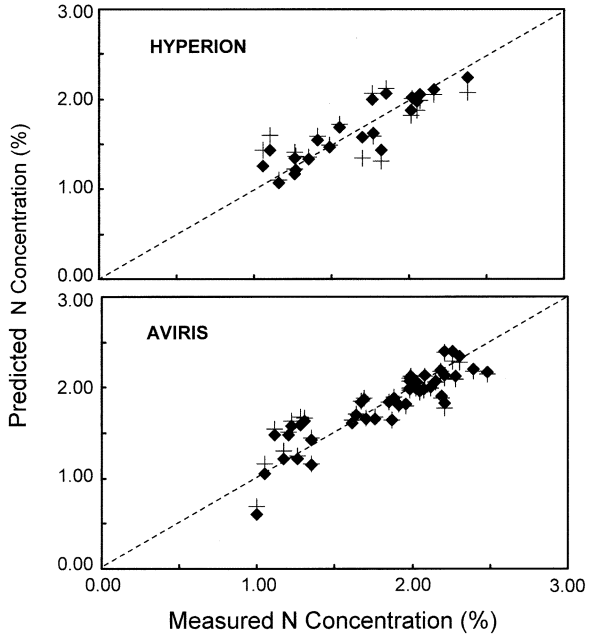

Fig. 2. Predicted versus measured canopy nitrogen concentration based on PLS regression models using (a) Hyperion and (b) AVIRIS absorbance data. In both panels, closed symbols represent the calibration model; open symbols represent the validation model; and dashed lines represent the 1 : 1 relationship.

tween-year correlation in N concentration among sample plots at BEF was strong and of a narrower range ($R^2 = 0.86$, SEE $= 0.17$, CV $= 0.10$; data in Table I). Thus, we are reasonably confident that foliar chemistry sampled in August 2000 is valid for use in calibration of Hyperion imagery collected the subsequent summer.

Table II summarizes PLS regression statistics for estimation of whole-canopy foliar N concentration from AVIRIS and Hyperion imagery. Fig. 2 shows the predicted versus measured canopy N concentration for the calibration and validation regression models for each image data source. Whole-canopy N concentration was best predicted from both AVIRIS and Hyperion imagery using a three-factor equation based on a first-derivative transformation of the absorbance data with a 1, 4, 3 math treatment applied.

Figs. 3 and 4 show wavelength loadings for significant PLS factors and regression coefficients derived from these factors that best predicted canopy N concentrations from AVIRIS and Hyperion first-derivative absorbance spectra, respectively. In the visible and near-infrared, wavelengths of highest loadings are centered between 0.48–0.80 μm, with important features near 0.48, 0.66, and 0.76 μm for AVIRIS spectra and at

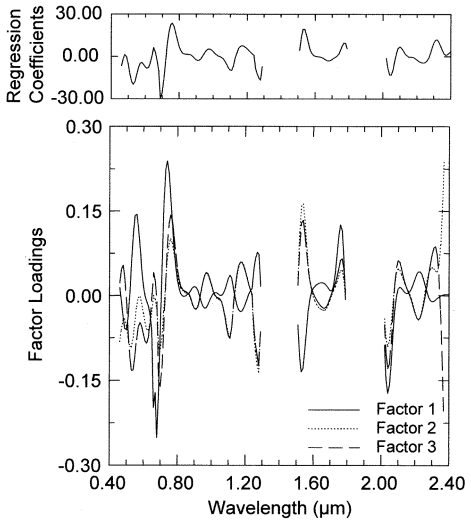

Fig. 3. Regression coefficients and factor loadings for a three-factor PLS regression model estimating nitrogen concentration of temperate forest canopies using first-derivative AVIRIS absorbance data.

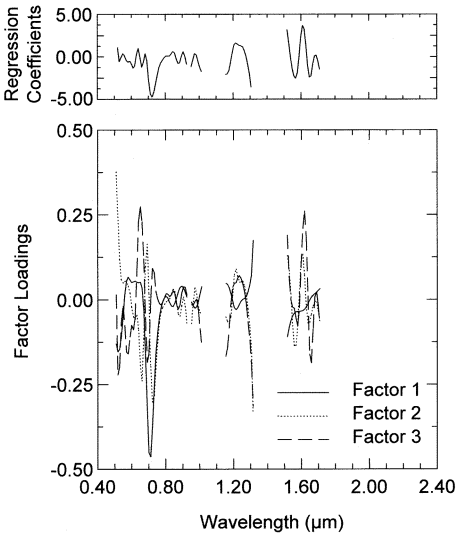

Fig. 4. Regression coefficients and factor loadings for a three-factor PLS regression model estimating nitrogen concentration of temperate forest canopies using first-derivative Hyperion absorbance data.

0.51, 0.64, 0.67, and 0.72 μm for Hyperion spectra. In the SWIR, a broad region between 1.19–1.28 μm and wavelengths between 1.51–1.69 μm (maxima at 1.51, 1.63, and 1.69 μm) are identified for Hyperion data. For AVIRIS, significant SWIR wavelengths include regions between 1.14–1.24 μm (maxima at 1.17 μm), 1.50–1.58 μm (maxima at 1.53), 1.71–1.79 μm (maxima at 1.74 μm), a broad feature from 2.06–2.18 μm, and 2.26–2.37 μm (maxima at 2.30 μm).

IV. DISCUSSION

Previous studies in temperate conifer and mixed deciduous forests have demonstrated that accurate empirical estimates of canopy chemistry, particularly nitrogen concentration, may be derived from aircraft-based high-altitude remote spectroscopic measurements [3]–[5], [25]–[27]. In this paper, we reconfirm this potential within north temperate forest canopies

for the ER-2-based AVIRIS instrument and, for the first time, demonstrate a similar potential for the space-based imaging spectrometer, Hyperion. Although Hyperion has a lower SNR and a narrower usable spectral range than the AVIRIS instrument, the accuracy of Hyperion-based prediction, as indicated by the validation regression RMSEP statistic (Table II), falls well within that needed to detect important spatial patterns of canopy nitrogen over native forest landscapes. Detection of canopy N within 0.5% by dry mass has been described as the minimum necessary to distinguish among ecosystems in their photosynthetic, and hence, productive potential [28]. Overall accuracy of Hyperion estimates were within 0.25% dry mass, and AVIRIS-based estimates were within 0.19% dry mass. Hyperion estimates, though of lower accuracy than AVIRIS-based estimates, are surprisingly robust given Hyperion's much lower SNR and the temporal offset between field data collection and image acquisition for the study site.

Leaf optical properties, and thus foliar chemistry, are expressed most strongly at the canopy level when canopies are optically dense. Combined field-data and canopy reflectance modeling studies suggest that canopy cover, leaf area, and leaf angle control the strength of biochemical expression in both the visible and near-infrared spectrum [29], [30]. Closed canopies of high leaf area and of generally horizontal leaf inclination, characteristics of the temperate and mixed coniferous forests examined in this study, best allow the generally weak leaf-level biochemical information, particularly in the NIR, to be enhanced at the canopy scale via multiple scattering [29].

Wavelength regions of high predictive value for detecting canopy nitrogen concentrations were largely consonant between AVIRIS and Hyperion spectral datasets (despite the temporal offset in image acquisition by the sensors and the difference in surface reflectance transformation), as well as with a number of previous empirically based studies. The most abundant nitrogen-bearing compounds in green leaves are proteins, mostly in the form of chlorophyll and of the carboxylating enzyme Rubisco [31]. Chlorophyll absorptions are due to electron transitions and are located in the visible region of the spectrum with primary features found near 0.43 and 0.66 μm (chlorophyll a) and 0.46 and 0.64 μm (chlorophyll b) [5].

In this study, absorption features at or near 0.66 μm were identified as important in both spectral datasets, as well as an AVIRIS feature at 0.48 μm and Hyperion features near 0.51 and 0.64 μm. Red-edge features at 0.76 μm in AVIRIS data and near 0.75 μm in Hyperion data were also identified. Red-edge features are known to vary with chlorophyll concentration and biomass amount, and have been identified in a number of previous imaging spectrometry studies as correlated with nitrogen concentration [26], [32].

Protein absorption features are found in the infrared portion of the spectrum and are due to harmonics and overtones of fundamental stretching frequencies of C–H, N–H, and O–H bonds at wavelengths in middle- and thermal-infrared regions. Primary absorption features associated with proteins are found near 1.02, 1.51, 1.68, 1.73, 1.98, 2.06, 2.13, 2.18, 2.24, and 2.30 μm [5], [6], [33].

In both datasets, the N–H stretch, first overtone near 1.51 μm (a primary absorption feature associated with protein and with nitrogen) was among those of highest factor loading. Similarly, a broad feature between 1.60 and 1.64 μm (C–H stretch first overtone associated with protein) was identified as important for the Hyperion data, with a smaller feature centered at 1.69 μm, as was the broad AVIRIS feature between 1.71 and 1.79 μm (C–H stretch, first overtone associated with protein). In aggregate, these spectral features are among the strongest absorption features for nitrogen in the SWIR region [5], [6] and have often been identified as important predictors of nitrogen in canopy-level imaging spectrometry studies [4], [32], [34], [35]. Additional features significant for the AVIRIS dataset include the 2.06–2.18–μm region and a peak at 2.30 μm related to N–H stretch and rotation features associated with protein and nitrogen absorption [5], [32].

Lower magnitude features identified between 0.90 and 1.02 μm and between 1.14 and 1.28 μm in both datasets are associated with minor water absorption features and with C–H stretch, second overtones common to all biochemical constituents [6].

The ability to scale field measurements from individual research plots to broader surrounding landscapes has long been a challenge to environmental scientists and resource managers. Over the past decade, the increasing awareness of processes that operate globally and the large data streams now generated from broad-scale remote sensing instruments (e.g., MODIS) has made this goal even more pertinent. Presently, our ability to interpret and evaluate the information gathered by regional- and continental-scale remote sensing instruments is substantially limited by the inherent incompatibility between plot-based field data and the kilometer-scale reflectance data generated by such instruments. Because hyperspectral sensors collect extensive amounts of spectral information and typically at spatial resolutions much more compatible with field measurements, their utility in detecting physiological canopy properties, such as canopy-level biochemistry, may represent a powerful way in which measurements and observations may be meaningfully linked across scales and among instruments.

ACKNOWLEDGMENT

The authors would like to thank N. Coops (CSIRO FFP) and D. Jupp (CSIRO EOC) for their help in understanding and preprocessing of Hyperion Level 1B data.

REFERENCES

[1] C. Field and H. A. Mooney, "The photosynthesis-nitrogen relationship in wild plants," in *On the Economy of Plant Form and Function*, T. Givnish, Ed. Cambridge, U.K.: Cambridge Univ. Press, 1986, pp. 22–55.

[2] P. B. Reich, D. S. Ellsworth, M. B. Walters, J. M. Vose, C. Gresham, J. C. Volin, and W. D. Bowman, "Generality of leaf trait relationships: A test across six biomes," *Ecology*, vol. 80, pp. 1955–1969, 1999.

[3] C. A. Wessman, J. D. Aber, D. L. Peterson, and J. M. Melillo, "Remote sensing of canopy chemistry and nitrogen cycling in temperate forest ecosystems," *Nature*, vol. 335, pp. 154–156, 1988.

[4] M. E. Martin and J. D. Aber, "High spectral resolution remote sensing of forest canopy lignin, nitrogen, and ecosystem processes," *Ecol. Appl.*, vol. 4, pp. 431–443, 1997.

[5] P. J. Curran, "Remote sensing of foliar chemistry," *Remote Sens. Environ.*, vol. 30, pp. 271–278, 1989.
[6] L. Kumar, K. Schmidt, S. Dury, and A. Skidmore, "Imaging spectrometry and vegetation science," in *Imaging Spectrometry*, F. D. van der Meer and S. M. de Jong, Eds. Dordrecht, The Netherlands: Kluwer, 2001, pp. 111–155.
[7] S. V. Ollinger, M. L. Smith, M. E. Martin, R. A. Hallett, J. D. Aber, and C. L. Goodale, "Regional variation in foliar chemistry and soil nitrogen status among forests of diverse history and composition," *Ecology*, vol. 83, pp. 335–339, 2002.
[8] M. L. Smith, S. V. Ollinger, M. E. Martin, J. D. Aber, R. A. Hallett, and C. L. Goodale, "Direct estimation of aboveground forest productivity through hyperspectral remote sensing of canopy nitrogen," *Ecol. Appl.*, vol. 12, pp. 1286–1302, 2002.
[9] K. L. Bolster, M. E. Martin, and J. D. Aber, "Determination of carbon fraction and nitrogen concentration in tree foliage by near infrared reflectance: A comparison of statistical methods," *Can. J. Forest Res.*, vol. 26, pp. 590–600, 1996.
[10] D. Ellsworth and P. B. Reich, "Canopy structure and vertical patterns of photosynthesis and related leaf traits in a deciduous forest," *Oecologia*, vol. 96, pp. 169–178, 1993.
[11] A. L. O'Neill, J. A. Kupiec, and P. J. Curran, "Biochemical and reflectance variation throughout a Sitka spruce canopy," *Remote Sens. Environ.*, vol. 80, pp. 134–142, 2002.
[12] M. L. Smith and M. E. Martin, "A plot based method for rapid estimation of forest canopy chemistry," *Can. J. Forest Res.*, vol. 31, pp. 549–555, 2001.
[13] R. O. Green, M. L. Eastwood, C. M. Sarture, T. G. Chrien, M. Aronsson, B. J. Chippendale, J. A. Faust, B. E. Pavri, C. J. Chovit, M. Solis, M. R. Olah, and O. Williams, "Imaging spectrometry and the Airborne/Visible Infrared Imaging Spectrometer (AVIRIS)," *Remote Sens. Environ.*, vol. 65, pp. 227–248, 1998.
[14] B. Gao, K. B. Heidebrecht, and A. Goetz, *Atmospheric Removal Program (ATREM) User's Guide*. Boulder, CO: Center for the Study of Earth From Space, Univ. Colorado, 1992.
[15] B. Gao, K. B. Heidebrecht, and A. Goetz, "Derivation of scaled surface reflectance from AVIRIS data," *Remote Sens. Environ.*, vol. 44, pp. 165–178, 1993.
[16] S. G. Ungar, J. S. Pearlman, J. Mendenhall, and D. Reuter, "Overview of the Earth Observing One (EO-1) mission," *IEEE Trans. Geosci. Remote*, vol. 41, pp. 1149–1159, June 2003.
[17] D. P. L. Jupp, B. Datt, J. Lovell, and E. King, "EO-1/Hyperion data workshop notes," CSIRO Office of Space Science and Applications, Earth Observation Centre, Canberra, Australia, Apr. 2002.
[18] *Acorn 4.0 User's Guide.*. Boulder, CO: Analytical Imaging and Geophysics, LLC.
[19] I. Murray and P. Williams, "Chemical principles of near-infrared technology," in *Near-Infrared Technology in the Agricultural and Food Industries*, 2nd ed, P. Williams and K. Norris, Eds. Saint Paul, MN: Amer. Assoc. Cereal Chemists, 1987, pp. 17–34.
[20] W. R. Hruschcka, "Data analysis: Wavelength selection methods," in *Near-Infrared Technology in the Agricultural and Food Industries*, 2nd ed, P. Williams and K. Norris, Eds. Saint Paul, MN: Amer. Assoc. Cereal Chemists, 1987, pp. 39–58.
[21] R. B. Myneni, F. G. Hall, P. J. Sellers, and A. L. Marshak, "The interpretation of spectral vegetation indexes," *IEEE Trans. Geosci. Remote Sensing*, vol. 33, pp. 481–486, Mar. 1995.
[22] CAMO Inc., The Unscrambler 7.6, CAMO Inc., Corvallis, OR, 2000.
[23] R. Kramer, *Chemometric Techniques for Quantitative Analysis*. New York: Marcel Dekker, 1998.
[24] A. H. Magill, J. D. Aber, G. M. Berntson, W. H. McDowell, K. J. Nadelhoffer, J. M. Mellilo, and P. Steudler, "Long-term nitrogen additions and nitrogen saturation in two temperate forests," *Ecosystems*, vol. 3, pp. 238–253, 2000.
[25] D. H. Card, D. L. Peterson, P. A. Matson, and J. D. Aber, "Prediction of leaf chemistry by the use of visible and near infrared spectroscopy," *Remote Sens. Environ.*, vol. 26, pp. 123–147, 1988.
[26] L. F. Johnson, C. A. Hlavka, and D. L. Peterson, "Multivariate analysis of AVIRIS data for canopy biochemical estimation along the Oregon transect," *Remote Sens. Environ.*, vol. 47, pp. 216–230, 1994.
[27] F. V. Zagoloski, J. Pinel, J. Romier, D. Alcayde, J. P. Gastellu-Etchegorry, G. Giordano, G. Marty, and E. Mougin, "Forest canopy chemistry with high spectral resolution remote sensing," *Int. J. Remote Sens.*, vol. 17, pp. 1107–1128, 1996.
[28] D. Schimel, "Terrestrial biogeochemical cycles: Global estimates with remote sensing," *Remote Sens. Environ.*, vol. 51, pp. 49–56, 1995.
[29] G. P. Asner, "Biophysical and biochemical sources of variability in canopy reflectance," *Remote Sens. Environ.*, vol. 64, pp. 234–253, 1998.
[30] J. P. Gastellu-Etchegorry and V. Bruniquel-Pinel, "A modeling approach to assess the robustness of spectrometric predictive equations for canopy chemistry," *Remote Sens. Environ.*, vol. 76, pp. 1–15, 2001.
[31] C. D. Elvidge, "Visible and near infrared reflectance characteristics of dry plant materials," *Int. J. Remote Sens.*, vol. 11, pp. 1775–1795, 1990.
[32] L. Serrano, J. Penuelas, and S. L. Ustin, "Remote sensing of nitrogen and lignin in Mediterranean vegetation from AVIRIS data: Decomposing biochemical from structural signals," *Remote Sens. Environ.*, vol. 81, pp. 355–364, 2002.
[33] D. S. Himmelsbach, J. D. Boer, D. E. Akin, and F. E. Bartion, "Solid state carbon-13 NMR, FTIR and NIR spectroscopic studies of ruminant silage digestion," in *Analytical Applications of Spectroscopy*, C. S. Creaser and A. M. C. Davies, Eds. London, U.K.: R. Soc. Chemistry, 1988, pp. 410–413.
[34] B. J. Yoder and R. E. Pettigrew-Crosby, "Predicting nitrogen and chlorophyll content and concentration from reflectance spectra (400–2500 nm)," *Remote Sens. Environ.*, vol. 53, pp. 199–211, 1995.
[35] S. J. Dury, X. Jia, and B. J. Turner, "From leaf to canopy: Determination of nitrogen concentration of eucalypt tree foliage using HyMap image data," in *Proc. 10th Australasian Remote Sensing and Photogrammetry Conference*, Adelaide, Australia, 2001, pp. 875–891.
[36] BEF, Unpublished data.

Marie-Louise Smith received the B.S. degree from the University of Michigan, Ann Arbor, in 1989, the M.S. degree in forestry from the University of Wisconsin, Madison, in 1992, and the Ph.D. degree in natural resources from the University of New Hampshire, Durham, in 2000.

Since 1992, she has been with the U.S. Department of Agriculture Forest Service, Northeastern Research Station, Durham, NH. Her research interests center on the potential of airborne and satellite-based imaging spectrometers to aid in remote detection of complex ecosystem processes such as forest productivity and biogeochemical cycling, and on field-based and modeling studies to examine important environmental controls on these processes.

Mary E. Martin received the B.S. degree in botany and the Ph.D. degree in natural resources from the University of New Hampshire, Durham.

Since 1998, she has been a Research Assistant Professor in the Complex Systems Research Center, University of New Hampshire, Durham. Her research has focused on the use of both laboratory and airborne hyperspectral data for the determination of foliar chemistry.

Lucie Plourde received the M.S. degree in natural resources from the University of New Hampshire, Durham.

She is currently a Research Scientist with the Complex Systems Research Center, University of New Hampshire, Durham. Her research involves hyperspectral and multspectral image analysis as well as GIS manipulations and applications to integrate remote sensing, canopy chemistry, and species composition for landscape-level forest ecosystem analyses.

Scott V. Ollinger received the B.S. degree in ecology and environmental science from the State University of New York, Purchase College, Purchase, in 1989 and the M.S. and Ph.D. degrees in natural resources from the University of New Hampshire, Durham, in 1992 and 2000, respectively.

Since 2000, he has been a Research Assistant Professor in the Institute for Earth, Oceans and Space (EOS), University of New Hampshire (UNH). Prior to joining the UNH EOS faculty, he served as a Research Scientist with the Complex Systems Research Center, UNH, from 1995 to 2000. His research interests span a variety of topics within the fields of ecology and biogeochemistry including carbon and nitrogen cycling, forest productivity and succession, plant-soil interactions, remote sensing, ecosystem modeling, and the effects of multiple environmental stressors on forests.